

# ATLAS MEASUREMENTS OF CP VIOLATION AND RARE DECAY PROCESSES WITH BEAUTY MESONS\* \*\*

ADAM BARTON

on behalf of the ATLAS Collaboration

Lancaster University, UK

*Received 28 September 2022, accepted 18 January 2023,  
published online 15 February 2023*

The ATLAS experiment at the LHC has performed measurements of  $B$ -meson rare decays proceeding via suppressed electroweak flavour changing neutral currents, and of mixing and CP violation in the neutral  $B_s$ -meson system. The focus is on the latest results from the ATLAS Collaboration, such as rare processes  $B_s^0 \rightarrow \mu\mu$  and  $B_d^0 \rightarrow \mu\mu$ , and CP violation in  $B_s \rightarrow J/\psi\phi$  decays. In the latter, the Standard Model predicts the CP violating mixing phase,  $\phi_s$ , to be very small and its SM value is very well constrained, while in many new physics models, large  $\phi_s$  values are expected. The latest measurements of  $\phi_s$  and several other parameters describing the  $B_s^0 \rightarrow \mu\mu$  decays will be reported.

DOI:10.5506/APhysPolBSupp.16.3-A1

## 1. Introduction

In this work, the authors present the current status of the ATLAS measurements of CP violation and rare decay processes with beauty mesons. ATLAS [1] is a general-purpose detector that measures heavy-flavour properties using its inner detectors, muon spectrometers, and electromagnetic calorimeters. Measuring the properties of heavy-flavour particles has been part of the  $B$ -physics program since the start of the proton–proton ( $pp$ ) collisions at the LHC in 2010. The analysis presented here [2] introduces a measurement of the  $B_s \rightarrow J/\psi\phi$  decay parameters using  $80.5 \text{ fb}^{-1}$  of LHC  $pp$  data collected by the ATLAS detector during 2015–2017 at a centre-of-mass energy,  $\sqrt{s}$ , equal to 13 TeV. The analysis closely follows a previous ATLAS

---

\* Presented at the XIV International Conference on *Beauty, Charm and Hyperon Hadrons*, Kraków, Poland, 5–10 June, 2022.

\*\* Copyright 2022 CERN for the benefit of the ATLAS Collaboration. Reproduction of this article or parts of it is allowed as specified in the CC-BY-4.0 license.

measurement [3] that was performed using  $19.2 \text{ fb}^{-1}$  of data collected at 7 TeV and 8 TeV, and introduces more precise models for both signal and backgrounds.

In the presence of New Physics (NP) phenomena, sources of CP violation in  $b$ -hadron decays can arise in addition to those predicted by the Standard Model (SM) [4]. In the  $B_s \rightarrow J/\psi\phi$  decay, CP violation occurs due to interference between a direct decay and a decay with  $B_s-\bar{B}_s^0$  mixing. The oscillation frequency of  $B_s$ -meson mixing is characterised by the mass difference  $\Delta m_s$  of the heavy ( $B_H$ ) and light ( $B_L$ ) mass eigenstates. The CP violating phase  $\phi_s$  is defined as the weak phase difference between the  $B_s-\bar{B}_s^0$  mixing amplitude and the  $b \rightarrow c\bar{c}s$  decay amplitude. In the SM the phase  $\phi_s$  is small and is related to the Cabibbo–Kobayashi–Maskawa (CKM) quark mixing matrix elements via the  $\phi_s \simeq -2\beta_s$  relation, with  $\beta_s = \arg[-(V_{ts}V_{tb}^*)/(V_{cs}V_{cb}^*)]$ . Assuming no NP contributions to  $B_s$  mixing and decays, a value of  $-2\beta_s = -0.0363_{-0.0015}^{+0.0016}$  rad can be predicted by combining beauty and kaon physics observables [5]. While large NP enhancements of the mixing amplitude have been excluded by the precise measurement of the oscillation frequency [6], the NP couplings involved in the mixing may still increase the size of the observed CP violation by enhancing the mixing phase  $\phi_s$  with respect to the SM value.

Flavour-changing neutral-current processes are highly suppressed in the SM. The branching fractions of the decays  $B_s^0 \rightarrow \mu^+\mu^-$  are helicity suppressed in the SM, and are predicted to be  $\mathcal{B}(B_s^0 \rightarrow \mu^+\mu^-) = (3.65 \pm 0.23) \times 10^{-9}$  and  $\mathcal{B}(B_d^0 \rightarrow \mu^+\mu^-) = (1.06 \pm 0.09) \times 10^{-10}$ . The second analysis I present is the result of a search for  $B_s^0 \rightarrow \mu^+\mu^-$  and  $B_d^0 \rightarrow \mu^+\mu^-$  decays performed using  $pp$  collision data corresponding to an effective integrated luminosity of  $26.3 \text{ fb}^{-1}$ , collected at 13 TeV centre-of-mass energy during the first two years of the LHC Run 2 data-taking period using the ATLAS detector. The analysis strategy follows that in Ref. [7].

## 2. ATLAS detector and data selection

The ATLAS detector consists of three main components: an inner detector (ID) tracking system immersed in a 2T axial magnetic field, electromagnetic and hadronic calorimeters, and a muon spectrometer (MS). The inner tracking detector covers the pseudorapidity range  $|\eta| < 2.5$ , and consists of silicon-pixel, silicon-micro-strip, and transition-radiation-tracking detectors. The ID is surrounded by a high-granularity liquid-argon (LAr) sampling electromagnetic calorimeter. A steel/scintillator tile calorimeter provides hadronic coverage in the central rapidity range. The MS surrounds the calorimeters and provides a system of tracking chambers and detectors for triggering. A full description can be found in Refs. [1, 8, 9].

The muon and tracking systems are of particular importance in the reconstruction of  $B_s$ -meson candidates. Only data collected when both these systems were operating correctly and when the LHC beams were declared to be stable are used in the analysis. The data were collected during periods with different instantaneous luminosity; therefore, several triggers were used in the analysis. All of them were based on the identification of a  $J/\psi \rightarrow \mu^+\mu^-$  decay, with transverse momentum ( $p_T$ ) thresholds of either 4 GeV or 6 GeV for the muons.

### 3. Maximum likelihood fit

An unbinned maximum-likelihood fit is performed on the selected events to extract the parameter values of the  $B_s \rightarrow J/\psi(\mu^+\mu^-)\phi(K^+K^-)$  decay. The fit uses information about the reconstructed mass  $m$ , the measured proper decay time  $t$ , the measured proper decay time uncertainty  $\sigma_t$ , the tagging probability, and the transversity angles  $\Omega$  of each  $B_s \rightarrow J/\psi\phi$  decay candidate. The measured proper decay time uncertainty  $\sigma_t$  is calculated from the covariance matrix associated with the vertex fit of each candidate event. The transversity angles  $\Omega = (\theta_T, \psi_T, \phi_T)$  are defined in Ref. [2], where further details can also be found.

### 4. Results

The full simultaneous unbinned maximum-likelihood fit contains nine physical parameters: decay width difference ( $\Delta\Gamma_s$ ), CP violating phase ( $\phi_s$ ), decay width ( $\Gamma_s$ ), transversity amplitudes ( $|A_0(0)|^2$ ,  $|A_{\parallel}(0)|^2$ ,  $|A_S(0)|^2$ ), and strong phases ( $\delta_{\parallel}$ ,  $\delta_{\perp}$ ,  $\delta_S$ ). The other parameters in the likelihood function are the  $B_s$  signal fraction  $f_s$ , parameters describing the  $J/\psi\phi$  mass distribution, parameters describing the decay time plus angular distributions of background events, parameters used to describe the estimated decay time uncertainty distributions for signal and background events, and scale factors between the estimated decay time uncertainties and their true uncertainties. In addition, there are also nuisance parameters describing the background and acceptance functions that are fixed at the time of the fit.

Multiplying the total number of events supplied to the fit with the extracted signal fraction and its statistical uncertainty provides an estimate for the total number of  $B_s$  meson candidates of  $477\,240 \pm 760$ . The results and correlations of the physics parameters obtained from the fit are given in Table 1. Fit projections of the mass and proper decay time are given in Fig. 1. and the  $\Delta\Gamma_s$  and  $\phi_s$  contours can be seen in Fig. 2.

Table 1. Values of the physical parameters extracted in the combination of 13 TeV results with those obtained from 7 TeV and 8 TeV data [2].

Parameter	Value	Statistical uncertainty	Systematic uncertainty
$\phi_s$ [rad]	-0.096	0.036	0.024
$\Delta\Gamma_s$ [ $\text{ps}^{-1}$ ]	0.070	0.004	0.003
$\Gamma_s$ [ $\text{ps}^{-1}$ ]	0.668	0.001	0.002
$ A_{\parallel}(0) ^2$	0.221	0.002	0.003
$ A_0(0) ^2$	0.518	0.001	0.004
$ A_S ^2$	0.041	0.003	0.006
$\delta_{\perp}$ [rad]	3.191	0.105	0.067
$\delta_{\parallel}$ [rad]	3.323	0.062	0.088
$\delta_{\perp} - \delta_S$ [rad]	-0.229	0.041	0.019

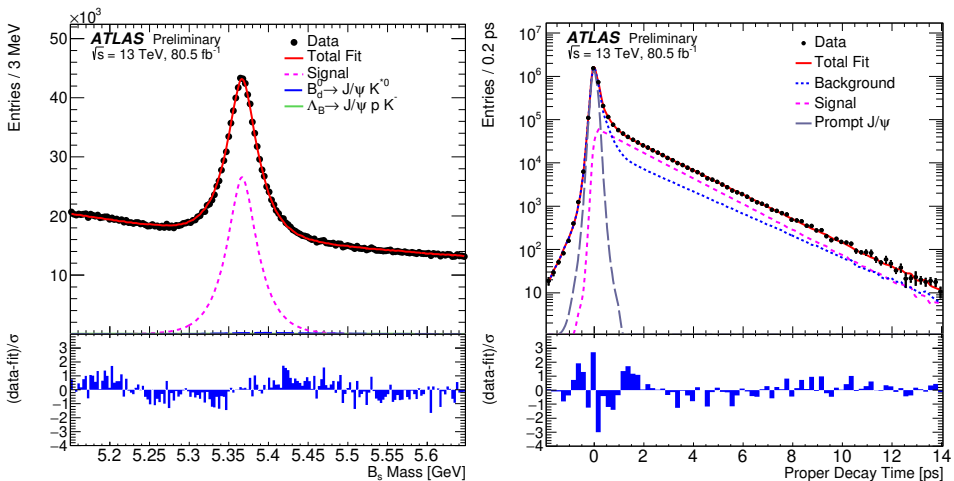


Fig. 1. Left: Mass fit projection for the  $B_s \rightarrow J/\psi\phi$  sample, from Ref. [2]. The red line shows the total fit, the dashed magenta line shows the  $B_s \rightarrow J/\psi\phi$  signal component, the blue line shows the  $B_d \rightarrow J/\psi K^{0*}$  component, while the green line shows the contribution from  $\Lambda_b \rightarrow J/\psi p K^-$  events. Right: Proper decay time fit projection for the  $B_s \rightarrow J/\psi\phi$  sample, from Ref. [2]. The red line shows the total fit, while the magenta dashed line shows the total signal.

The values from the 13 TeV analysis are consistent with those obtained in the previous analysis using 7 TeV and 8 TeV ATLAS data [3].

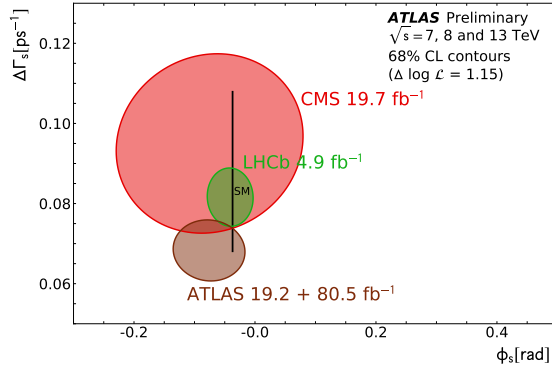


Fig. 2. Likelihood 68% confidence level contours in the  $\phi_s - \Delta\Gamma_s$  plane, including results from the LHCb [10] (green) and CMS [11] (red) using 7 TeV and 8 TeV data. The brown contour shows the ATLAS [2] result for  $\sqrt{s} = 13$  TeV combined with the results for  $\sqrt{s} = 7$  TeV and 8 TeV. In all contours, the statistical and systematic uncertainties are combined in quadrature. Figure from Ref. [2].

## 5. $B \rightarrow \mu\mu$ results

The likelihood function from the Run 2 result is combined with the likelihood function from the Run 1 result. A negligible change in the results, corresponding to shifts in central values and uncertainties between 1% and 4%, is found when all sources of systematic uncertainty are assumed to be fully correlated.

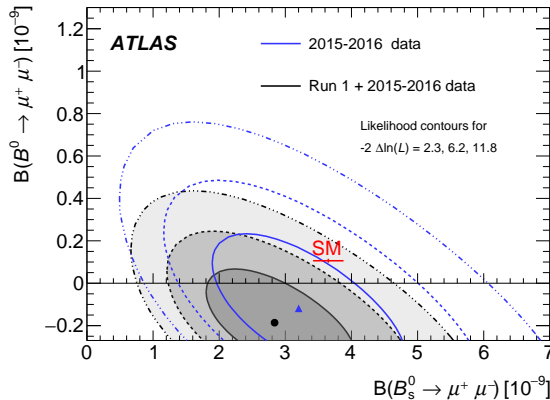


Fig. 3. Likelihood contours for the combination of the Run 1 and 2015–2016 Run 2 results (shaded areas). The contours are obtained from the combined likelihoods of the two analyses, for values of  $-2\Delta\ln(L)$  equal to 2.3, 6.2, and 11.8. The empty contours represent the result from 2015–2016 Run 2 data alone. The SM prediction with uncertainties is indicated [7].

The maximum of the combined likelihood corresponds to  $\mathcal{B}(B_s^0 \rightarrow \mu^+ \mu^-) = (2.8 \pm 0.7) \times 10^{-9}$  and  $\mathcal{B}(B^0 \rightarrow \mu^+ \mu^-) = (-1.9 \pm 1.6) \times 10^{-10}$ . Figure 3 shows the likelihood contours for the combined Run 1 and Run 2 result.

## 6. Conclusion

ATLAS has competitive results in  $B$ -physics, CP violation, and rare decay processes with beauty mesons. The collaboration is working on the updates to the mentioned analysis to full Run 2 statistics and is well prepared for the LHC Run 3 data.

## REFERENCES

- [1] ATLAS Collaboration, *J. Instrum.* **3**, S08003 (2008).
- [2] ATLAS Collaboration, *Eur. Phys. J. C* **81**, 342 (2021).
- [3] ATLAS Collaboration, *J. High Energy Phys.* **1608**, 147 (2016).
- [4] F.J. Botella, G.C. Branco, M. Nebot, *Nucl. Phys. B* **768**, 1 (2007).
- [5] J. Charles *et al.*, *Phys. Rev. D* **84**, 033005 (2011).
- [6] LHCb Collaboration, *New J. Phys.* **15**, 053021 (2013),  
[arXiv:1304.4741](https://arxiv.org/abs/1304.4741) [[hep-ex](#)].
- [7] ATLAS Collaboration, *J. High Energy Phys.* **2019**, 098 (2019).
- [8] B. Abbott *et al.*, *J. Instrum.* **13**, T05008 (2018),  
[arXiv:1803.00844](https://arxiv.org/abs/1803.00844) [[physics.ins-det](#)].
- [9] ATLAS Collaboration, «ATLAS Insertable B-Layer Technical Design Report», ATLAS-TDR-19, 2010, <https://cds.cern.ch/record/1291633/>
- [10] LHCb Collaboration, *Phys. Rev. Lett.* **114**, 041801 (2015),  
[arXiv:1411.3104](https://arxiv.org/abs/1411.3104) [[hep-ex](#)].
- [11] CMS Collaboration, *Phys. Lett. B* **757**, 97 (2016).